Proc. Natl. Acad. Sci. USA
Vol. 87, pp. 5430–5434, July 1990
Biophysics

Distribution and self-organization of photosynthetic pigments in micelles: Implication for the assembly of light-harvesting complexes and reaction centers in the photosynthetic membrane

(bacteriochlorophyll/aggregation/Poisson distribution/free-energy change)

A. SCHERZ†, V. ROSENBACH-BELKIN, AND J. R. E. FISHER

Department of Biochemistry, The Weizmann Institute of Science, Rehovot 76100, Israel

Communicated by George Feher, January 8, 1990 (received for review September 18, 1989)

ABSTRACT **The addition of bacteriochlorophylls and bacteriopheophytins to formamide/water, 3:1 (vol/vol), (or water) containing small spherical micelles of Triton X-100 leads to the reorganization of the detergent into micelles that consist of 5000–40,000 amphiphilic molecules. The pigment distribution within the micelles was determined by modified Poisson statistics taking into consideration the various sizes of micelles. Pigment dimerization occurred in micelles with more than a single occupant and was driven by a free-energy change of −4.5 kcal/mol (1 cal = 4.184 J) for bacteriochlorophyll a in formamide/water, −7.6 kcal/mol for bacteriopheophytin a in formamide/water, and −6.6 kcal/mol for bacteriopheophytin a in water. These values correspond to the room temperature equilibrium constants 2.2 × 10^3 M^{-1}, 3.9 × 10^5 M^{-1}, and 7.5 × 10^4 M^{-1}, respectively. The incorporation of bacteriochlorophylls with attached small formamide polymers and the subsequent dimerization of these pigments in the lipid phase provide a model for studying the synergetic organization of polypeptides and bacteriochlorophyll clusters in the photosynthetic membrane.**

Biological photosynthesis converts solar energy into a useful electrical potential. This solar energy conversion is carried out by the joint action of membrane-bound pigment proteins termed light-harvesting complexes (LHCs) and reaction centers (RCs) (1). Each organism contains several forms of LHCs that are packed around the RC. With a long wavelength for maximum absorption, the RC provides a kinetic trap for photons that are funneled from the LHCs (2). These trapped photons are then used to drive a charge separation across the photosynthetic membrane (1).

The diverse absorptions of the various LHCs and RCs originate from a few hydroporphyrin constituents: chlorophylls (Chls) in oxygenic organisms and bacteriochlorophyll (Bchl) in nonoxygenic bacteria (2). Since these pigments are not chemically modified by their respective protein environment, their spectral versatility is primarily a result of the *in vivo* setting (3). Most Chls and Bchls form clusters that are noncovalently attached to membrane proteins (2, 4). In these pigment–protein complexes, there is approximately one Chl (Bchl) molecule for every 4–8 kDa of protein. The separation between individual pigments can be as small as 3.2–3.4 Å (face-to-face) (4–7). At such distances, one would expect interactions among both the ground- and photo-excited states of the molecules involved (8, 9). For the primary electron donors in purple bacteria (P-860 and P-960), it is generally agreed that interactions among the excited states of the coupled Bchls depend upon the geometry of the chromophores and lead to part of the bathochromic shift of the lowest energy (Q_y) transition, as compared with the isolated pigments *in vitro* (9–12). However, the elements involved in determining the chromophore geometry have not yet been elucidated.

Earlier studies have primarily focused on the donor–acceptor interactions between the keto group of one chromophore and the central Mg of another, whereas the possible affect of chromophore attachment to the protein network has generally been ignored (13–21). The critical factors in the donor–acceptor type of dimerization are (*i*) the extent to which extraneous nucleophiles (e.g., H_2O) compete for coordination with the Mg and (*ii*) the availability of the keto group (18). Raman spectroscopy (22) and x-ray crystallography (4–7) studies of bacterial RCs have indicated that most of the *in vivo* Chls and Bchls are hydrogen-bonded at their carbonyl functions and strongly ligated to the protein network at their central Mg. Therefore, if Chls and Bchls self-assemble *in vivo*, they do not rely upon interactions among these sites but, rather, upon π–π interactions. This type of interactions has been observed for various nonhydroporphyrins (23) and Chls (24) and, recently, for various Bchls, bacteriopheophytins (Bphes), and Chls in aqueous solutions (3, 25–30). Once the Chls and Bchls are attached to single polypeptides, their self-dimerization may affect the formation of protein networks in the LHCs and RCs.

A 3:1 (vol/vol) formamide/water solution (FW) was found to be conducive for the self-organization of various Chls and Bchls into large oligomers with spectral properties similar to those observed *in vivo* (25–31). Even though FW is hydrophilic, it imitates the *in vivo* pigment environment in two ways: (*i*) the formamide forms polymer chains that resemble the polypeptide backbone (32) and (*ii*) these polymer chains provide groups for hydrogen-bonding with the Bchl molecules. The η transition around 340 nm is evidence that the isocyclic carbonyl oxygen of the Bchl is hydrogen-bonded to the solvent (27, 33).

To achieve a more realistic assay of the photosynthetic pigment organization, we explored the possibility of having hydroporphyrins with attached formamide and water molecules aggregate into small oligomers in a hydrophobic medium. Micellar solutions seem to be most suitable since each micelle forms a hydrophobic microenvironment in which a limited number of chromophores can be incorporated. Therefore, the micelles resemble the lipid environment in which the protein–chromophore complexes are situated *in vivo* (34).

The addition of native Chls, Bchls, and their synthetic derivatives to the micellar system usually results in two spectral forms: (*i*) a short wavelength-absorbing (S) form that resembles the monomers of the particular porphyrin in or-

The publication costs of this article were defrayed in part by page charge payment. This article must therefore be hereby marked "*advertisement*" in accordance with 18 U.S.C. §1734 solely to indicate this fact.

Abbreviations: Bchl, bacteriochlorophyll; Bphe, bacteriopheophytin; LHC, light-harvesting complex; RC, reaction center; TX-100, Triton X-100; Chl, chlorophyll; S and L, short- and long-wavelength absorbing forms, respectively.

†To whom reprint requests should be addressed.

ganic solvents containing traces of nucleophiles and (*ii*) a long wavelength-absorbing (L) form that resembles the particular pigment *in vivo* (3, 25–31). When the spectral properties of Bchl in the FW/Triton X-100 (TX-100) system was explored, the L form was found to be a dimer that resembled P-860 and the pigment centers in the LHC B850 (28, 35). The optical absorption and circular dichroism in all three systems were apparently determined by chromophore–chromophore interactions within Bchl dimers of the same geometry.

Herein we report on the detailed assembly of these dimers and those of bacteriopheophytin a (Bphe-a) within the TX-100 micelles. In doing so, we hope to understand the role of Chls (Bchls) during the polypeptide's incorporation into the lipid membrane and further assembly into protein matrices (36).

MATERIALS AND METHODS

Bchl-a was extracted and purified from whole *Rhodospirillum rubrum* cells as described (3, 25–28). Bphe-a was prepared by acidification of dry Bchl-a with acetic acid (3).

Incorporation of Bchls and Bphes into TX-100 micelles was carried out by mixing 1 vol of FW (or water) containing the pigments with 1 vol of FW (or water) containing the detergent (28).

Pigment association or dissociation was monitored by optical and circular dichroism (CD) spectroscopy as described (28).

RESULTS AND DISCUSSION

There are two spectral forms of Bchl-a in FW containing TX-100 (28). One form (Fig. 1*A*, dashed line) has a shorter wavelength for maximum absorption than the other (Fig. 1*A*, solid line). The former (denoted by S) is probably a Bchl-a monomer solubilized by TX-100 micelles, and the latter (denoted by L) is probably a Bchl-a dimer (28). This dimer shows spectral and structural resemblance to the primary electron donor P-860 and the LHC B850 in purple bacteria (28). Similar spectral forms were observed when FW (or water) containing Bphe-a was added to FW (or water) containing TX-100 (Fig. 1*B*). To calculate the concentration of Bphe-a and Bchl-a in each spectroscopic form, we used their extinction coefficients (25, 28). For both pigment molecules, the ratio between the two spectral forms at equilibrium depended upon the concentration of the TX-100 and the total pigment concentration: at high pigment or low TX-100 concentrations the L form was dominant. The dependence of [S] and [L] on the total pigment concentration is shown in Fig. 2.

We have shown (28) that the S and L forms of Bchl-a are congruent with monomers and dimers, respectively, throughout a relatively large range of concentrations (5×10^{-7} M to 1×10^{-5} M). When considering the apparent equilibrium between the two forms, the system was divided into two domains: the aqueous solution outside the micelles and the micellar phase (28). However, it should, in fact, be divided into at least three domains: micelles containing two or more pigment molecules, micelles containing only one pigment molecule, and the aqueous solution outside the micelles. In the last domain the pigment behaves in a cooperative manner, as described (25, 29, 31); namely, as long as the pigment concentration is less than a critical value given by K_b^{-1}, this domain will be populated solely by monomers. When this criterion is met, equilibrium occurs exclusively between

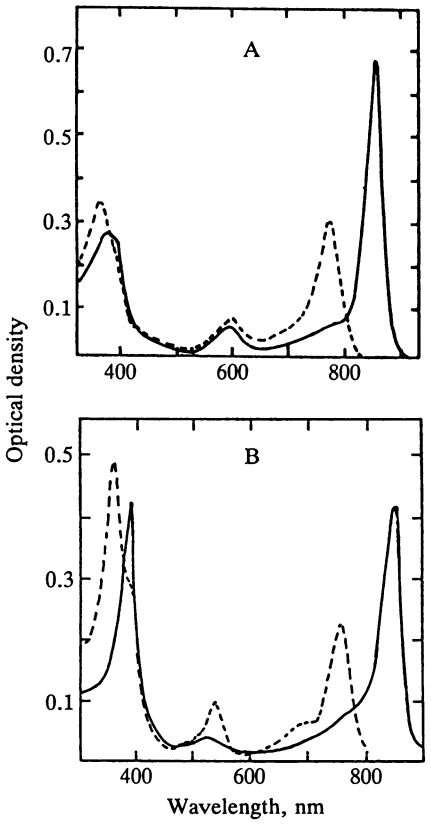

FIG. 1. (*A*) Absorption spectra of 5.2 μM L form Bchl-a (—) and 5.0 μM S form Bchl-a (---) in FW containing 6 mM TX-100 and 50 mM TX-100, respectively. (*B*) Absorption spectra of 3.7 μM L form Bphe-a (—) and 3.8 μM S form Bphe-a (---) in FW containing 12 mM TX-100 and 0.12 M TX-100, respectively.

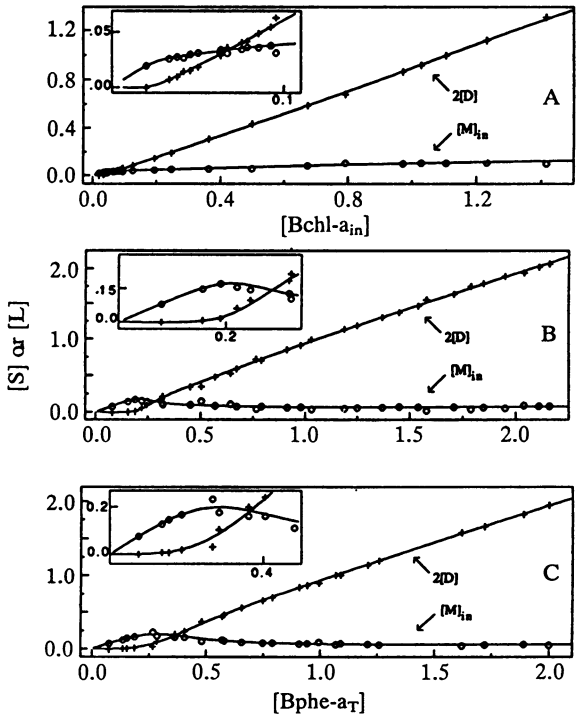

FIG. 2. Experimental concentrations of the L (+) and S (○) form Bchl-a and Bphe-a and the corresponding 2[D] and [M_{in}] (solid lines) calculated from Eqs. 7 and 9. (*A*) Bchl-a in FW (in the calculated curve [TX*] = 2.45 mM; $K_d = 2.2 \times 10^3$ M^{-1}; $Z = 4100$; and $C = 8 \times 10^{-8}$). (*B*) Bphe-a in FW (in the calculated curve [TX*] = 98.3 mM; $K_d = 3.9 \times 10^5$ M^{-1}; $Z = 40{,}000$; and $C = 4.5 \times 10^{-7}$). (*C*) Bphe-a in water (in the calculated curve [TX*] = 11.7 mM; $K_d = 7.5 \times 10^4$ M^{-1}; $Z = 4000$; and $C = 1 \times 10^{-6}$). [The critical micelle concentration for TX-100 was taken as 3.66 mM in FW (28) and 0.5 mM in water (37).] Units for [S], [L], [Bchl-a_{in}], or [Bphe-a_T] are M $\times 10^5$.

dimers and monomers in the first domain. Since all the dimers in solution are found in this domain, their concentration can be calculated directly from the spectra. The monomers, however, must be divided into three categories corresponding to the three domains: the monomers in the first domain (M*), the monomers that occupy the micelles as single occupants (M_{single}), and the monomers in the aqueous solution outside the micelles (M_{out}). Only the M* monomers directly participate in dimerization. The constant ratio between $[M_{out}]$ and the concentration of monomers inside the micelle ($[M_{in}]$) enabled us to calculate the contribution of $[M_{out}]$ to the total monomer concentration (28). The other two types of monomers could be expressed as functions of the total pigment concentration inside the micelle ($[B_{in}]$), where $[B_{in}]$ is given by

$$[B_{in}] = 2[D] + [M^*] + [M_{single}], \quad [1]$$

and 2[D] represents the concentration of the L-form molecules.

To determine the concentration of monomers in the singly occupied micelles ($[M_{single}]$), we utilized the formula for Poisson distribution,‡

$$P(A, I) = \frac{(A^I e^{-A})}{I!}, \quad [2]$$

where P is the probability of having a micelle populated by I pigment molecules and A is the ratio of the total pigment concentration inside the micelles to the micelle concentration. When $I = 1$, P represents the probability that a monomer will be a single occupant in a micelle. Multiplying this probability by the micelle concentration ([MT]) gave the concentration of such monomers;

$$[M_{single}] = [MT]([B_{in}]/[MT])\exp(-[B_{in}]/[MT]). \quad [3]$$

To express the monomers in the first domain ([M*]) in terms of $[B_{in}]$, it was necessary to derive the equilibrium equation within the micelles. The apparent equilibrium constant K'_d is given by

$$K'_d = [D]/[M^*]^2. \quad [4]$$

The concentrations referred to here are given with respect to the entire volume of the solution but, as was mentioned above, under the experimental conditions dimerization occurred in only part of this volume; namely, the volume occupied by the micelles of the first domain. Therefore, to calculate the true dimerization constant (K_d), it was necessary to transform [M*] and [D] from mol per total volume into mol per first-domain volume.

From the fluorescence quenching of Bchl in FW/TX-100, it was concluded that each micelle contained several thousand molecules of TX-100 (28). Micelles of this size presumably form long cylinders. Therefore, the volume factor (F) or the volume occupied by the micelles in the first domain (V_1) per liter (10^{27} Å^3) of FW, is given by

$$F = \frac{V_1}{\text{liter}} = \left[\frac{[TX^*]a}{[MT]2\pi R}\right]\left(\pi R^2 \frac{N}{10^{27}}\right) \times \left\{[MT] - ([B_{in}] + [MT])\exp\left(-\frac{[B_{in}]}{[MT]}\right)\right\}, \quad [5]$$

where [TX*] is the concentration of TX-100 less the critical micelle concentration, a is the surface area of the TX-100 hydrophilic head (taken here as 20 Å^2), R is the average length of the TX-100 molecule [taken here to be 35 Å (39)], N is Avogadro's number (6.02×10^{23} molecules per mol), and the factor 10^{27} converts Å^3 into liters. The first term in brackets expresses the height of the cylindrical micelles, which is then multiplied by the base area of the micelle and the number of first-domain micelles per liter. Dividing the monomer and dimer concentrations by this factor gave their concentration within the volume V_1, so that the true equilibrium equation became

$$K_d = \frac{[D]}{[M^*]^2} \times \frac{[TX^*]aR6.02\left\{[MT] - ([B_{in}] + [MT])\exp\left(-\frac{[B_{in}]}{[MT]}\right)\right\}}{2[MT] \times 10^4}. \quad [6]$$

By using the latter equation, the dimer concentration was expressed as a function of [M*] and K_d;

$$[D] = \frac{2K_d[M^*]^2[MT] \times 10^4}{[TX^*]aR6.02\left\{[MT] - ([B_{in}] + [MT])\exp\left(-\frac{[B_{in}]}{[MT]}\right)\right\}}. \quad [7]$$

Substituting this expression for [D] and the expression for $[M_{single}]$ (Eq. 3) in the equation for $[B_{in}]$ (Eq. 1) resulted in a quadratic with respect to [M*]. Adding this expression for [M*] to the expression for $[M_{single}]$, given by Eq. 3, provided a formula for simulating the monomer concentration inside the micelles given a certain K_d, [TX*], and [MT].

Until now, we have assumed that the micelles have a unique size depending only on the solvent system; however, this is not necessarily true. Kushner and Hubbard (39) found that micelles of TX-100 that formed in water consisted of 150 molecules, whereas Scherz and Rosenbach-Belkin (28) found that micelles containing pigment molecules consisted of ≈5000 amphiphilic molecules (for Bchl-a in FW). A similar size discrepancy was observed when lauryl dimethylamine oxide micelles were formed in the presence and absence of Bphe-a (3). This could mean that there was a distribution of micelle sizes whereby the size depended upon the number of pigment molecules within the micelle.

To find the true micelle concentration, we assumed that [TX*] is arranged into two forms; small empty micelles that consist of 150 amphiphilic molecules (38) and large populated micelles that, when averaged, consist of Z molecules. The probability for the TX-100 to form empty micelles can be estimated using Poisson's formula (Eq. 2) and substituting a virtual micelle concentration C for [MT]. Likewise, the probability for the TX-100 to form occupied micelles is one minus the probability to form empty micelles. So that, the total micelle concentration is the sum of the concentrations of each micelle form

$$[MT] = (1/150)\,[TX^*]\exp(-[B_{in}]/C) + (1/Z)\,[TX^*]\{1 - \exp(-[B_{in}]/C)\}. \quad [8]$$

Incorporating this varying micelle concentration into the sum of $[M_{singles}]$ and [M*] resulted in an expression for $[M_{in}]$ that should fit the experimental concentration of S throughout the entire range of $[B_{in}]$.

$$[M_{in}] = (F/4K_d) \times (-1 + [1 + 4(2k_d/F)[B_{in}]\{1 - \exp(-[B_{in}]/[MT])\}]^{1/2}) + [B_{in}]\exp(-[B_{in}]/[MT]). \quad [9]$$

‡In using this formula, we have assumed that the pigment molecules populate the micelles in a random manner and independent of other existing occupants.

where F is given by Eq. **5**, [MT] is given by Eq. **8**, and K_d, Z, and C are independent variables. Fig. 3 shows the dependence of $[M_{in}]$ and 2[D] on $[B_{in}]$ for various values of K_d, Z, and C. Each of these parameters affected the curves in a distinct manner and in a different range of $[B_{in}]$. This property of the equation was beneficial when fitting the experimental [S] and [L] values with the theoretical $[M_{in}]$ and 2[D] curves.

To fit the experimental values of [S] and [L] (Fig. 2) with $[M_{in}]$ and 2[D], respectively, it was necessary to find the corresponding $[B_{in}]$ values. For Bchl-a, one-fifth of the monomers remained in the FW domain (28).§ Therefore, $[B_{in}]$ was given by

$$[\text{Bchl-a}_{in}] = [\text{Bchl-a}_T] - \frac{1}{5}[\text{Bchl-a}_{monomer}], \qquad [10]$$

where $[\text{Bchl-a}_{monomer}]$ is the total concentration of Bchl-a monomers calculated from their maximum absorption at 780 nm (28) and $[\text{Bchl-a}_T]$ is the total concentration of Bchl-a molecules in all forms.

The threshold concentration for the formation of the large Bphe-a aggregates in FW is $\approx 10^{-9}$ M (27, 29, 38). By following the same arguments presented for $[\text{Bchl-a}_{out}]$ (28), we deduced that the Bphe-a molecules predominantly resided inside the micellar domain. Hence, the concentration of Bphe-a occupying the micelles ($[\text{Bphe-a}_{in}]$) was approximately equal to $[\text{Bphe-a}_T]$.

Once the experimental concentrations were plotted against their appropriate $[B_{in}]$ values, we searched for values of K_d, Z, and C that, when substituted into Eqs. **7** and **9**, provided [D] and $[M_{in}]$ values that fit the experimental points. The best fit was found for the Bchl-a system when $K_d = 2.2 \times 10^3\ M^{-1}$, for the Bphe-a in the FW system when $K_d = 3.9 \times 10^5\ M^{-1}$, and for the Bphe-a in the water system when $K_d = 7.5 \times 10^4\ M^{-1}$. The corresponding free-energy change (ΔG) for each system was −4.5 kcal/mol for Bchl-a, −7.6 kcal/mol for Bphe-a in FW, and −6.6 kcal/mol for Bphe-a in water. The appropriate Z values were 4100 TX-100 molecules for micelles occupied by Bchl-a, 40,000 molecules for micelles occupied by Bphe-a in FW, and 4000 molecules for micelles occupied by Bphe-a in water. The micelle size was also dependent upon the concentration of TX-100, which was different in each case (Fig. 2). The suitable C values for each system are given in Fig. 2.

The concentration dependence of the Bphe-a monomers on the total pigment content in solutions of water and FW containing TX-100 (Fig. 2) resembled the concentration dependence of the same molecule in a water/acetic acid solution containing lauryl dimethylamine oxide (3). In all systems, the incorporation of Bphe-a molecules into small spherical micelles promoted the formation of very large cylindrical micelles and the concomitant dimerization of the pigments.

Analyses of the time-dependent spectrum of Bphe-a molecules after their incorporation into the TX-100 micelles (Fig. 4) provided further evidence for pigment dimerization and pigment-induced micelle reorganization. The time lag observed before formation of L-form Bphe-a molecules was probably because the majority of pigment molecules were single occupants of small micelles. Once the micelles begin to reorganize into very large cylinders, [MT] decreases, $[M_{singles}]$ decreases, and [M*] increases. Finally, the Bphe-a molecules existed as multiple occupants within the large cylindrical micelles and the process of dimerization occurred with a second-order rate constant, $k_d = 1.18 \times 10^3\ min^{-1}$ (Fig. 4*B*).

§Scherz and Rosenbach-Belkin (28) used $K_s[MT] = 4$ when describing the ratio of monomers inside the micellar domain to monomers in the aqueous domain. However, this expression is not correct because in the present study we have found that at low pigment concentrations [MT] varies. Therefore, a more realistic expression for the partitioning of the pigments between the two phases (aqueous and micellar) should be $K_s'[TX^*] = 4$.

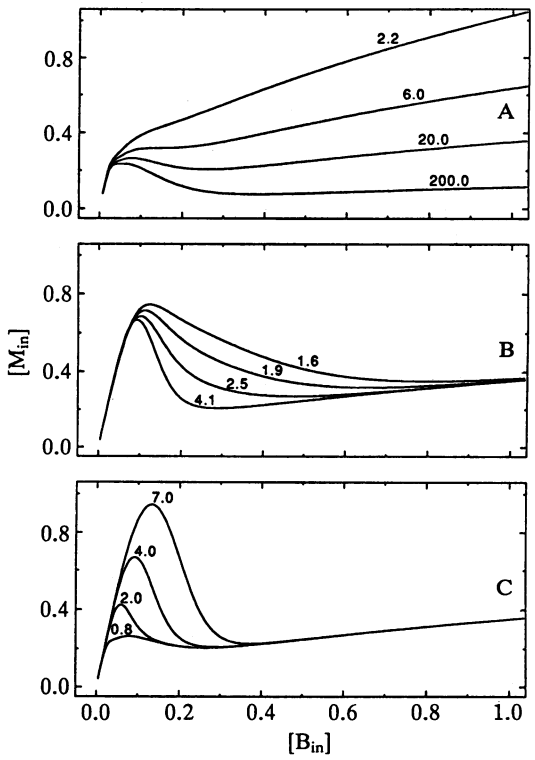

FIG. 3. Theoretical monomer concentration ($[M_{in}]$) versus $[B_{in}]$ calculated for [TX*] = 2.45 mM and a small micelle size of 150 molecules. (*A*) $Z = 4100$, $C = 8 \times 10^{-8}$, and K_d is varied by the values shown ($\times 10^3\ M^{-1}$). (*B*) $K_d = 2.0 \times 10^4\ M^{-1}$, $C = 4 \times 10^{-7}$, and Z is varied by the values shown ($\times 10^3$). (*C*) $K_d = 2.0 \times 10^4\ M^{-1}$, $Z = 4100$, and C is varied by the values shown ($\times 10^{-7}$). Units for $[M_{in}]$ are $M \times 10^6$ and units for $[B_{in}]$ are $M \times 10^5$.

CONCLUDING REMARKS

Until recently, the photosynthetic pigments were thought to play a passive role in the assembly of LHCs and RCs. Their tuning to the prevailing light conditions and their synchronization to each other were thought to be the result of specific effects of the protein environment (2, 37). The significance of pigment self-assembly was completely ignored once it was discovered that the pigments are bound to the polypeptide networks. However, investigation of LHC and RC biogenesis indicated that the Chls and Bchls are essential to the assembly of the protein network (36). For example, the heavy, light, and medium-sized subunits of the RC in bacteria are transcribed, translated, and attached to the intracytoplasmic membrane but are not incorporated or assembled when the Bchls with their esterified alcohols are absent (36).

In the present study, we have shown that Bchls and Bphes with attached FW chains are easily incorporated into the lipid micelles. Once inside the lipid matrix, their relative concentration increases by several orders of magnitude. Driven by a high free-energy change (−4 to −6 kcal/mol), the pigment–FW structures dimerize and consequently undergo a profound change in their spectral properties. Considering the similarities between the formamide chain and the polypeptide backbone, as well as the TX-100 micellar environment and the lipid membrane, we put forth this system as a model for studying several aspects of the incorporation and assembly of the photosynthetic pigments and polypeptides in the intra-

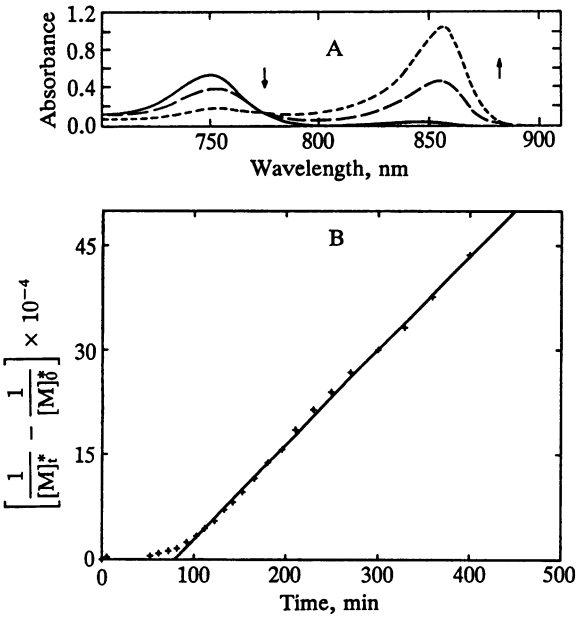

FIG. 4. (*A*) Spectrum of Bphe-a in FW containing 77.5 mM TX-100: 5 min after preparation (—), 4 hr after preparation (– – –), and 24 hr after preparation (-----). (*B*) Time dependence of Bphe-a monomers in the same system at various times after preparation. $[M]_t^*$ is the concentration of monomers that occupy TX-100 micelles with at least one other pigment molecule at time t and $[M]_0^*$ equals [M*] at time zero. The dimerization rate constant is given by $k_d = d(1/[M^*])/dt$.

cytoplasmic membrane. Consequently, we propose the following scheme. The attachment of Bchl or Chl to the single polypeptides of the LHCs or RCs facilitates their insertion into the intracytoplasmic membrane. Reorganization of the lipid membrane induced by the incorporated pigment polypeptides accelerates the insertion of additional units. The large increase of the local Bchl concentration in the lipid membrane (i.e., the Bchl concentration in the RC is $\approx 2 \times 10^{-2}$ M) plus the van der Waals forces among the amino acid residues (39) causes the self-assembly of several incorporated pigment polypeptides. At the same time, the formation of pigment dimers leads to a bathochromic shift of the pigment's lowest energy transition.

A.S. is the incumbent of the Recanati Career Development chair. This work is partial fulfillment of the Ph.D. thesis for V.R.-B. and of the M.Sc. thesis for J.R.E.F.

1. Okamura, M. Y., Feher, G. & Nelson, N. (1982) in *Photosynthesis, Energy Conversion by Plants and Bacteria*, ed. Govindjee (Academic, New York), pp. 221–227.
2. Zuber, H. (1985) *Photochem. Photobiol.* **42**, 821–844.
3. Scherz, A. & Parson, W. W. (1984) *Biochim. Biophys. Acta* **766**, 653–665.
4. Deisenhofer, J., Epp, O., Miki, K., Huber, R. & Michel, H. (1985) *Nature (London)* **318**, 618–624.
5. Chang, H., Tiede, D., Tang, J., Smith, U., Norris, J. R. & Schiffer, M. (1986) *FEBS Lett.* **205**, 82.
6. Allen, J. P., Feher, G., Yeates, T. O., Komiya, H. & Rees, D. C. (1987) *Proc. Natl. Acad. Sci. USA* **84**, 5730–5734.
7. Allen, J. P., Feher, G., Yeates, T. O., Komiya, H. & Rees, D. C. (1987) *Proc. Natl. Acad. Sci. USA* **84**, 6162–6166.
8. Scherz, A. & Parson, W. W. (1984) *Biochim. Biophys. Acta* **766**, 666–678.
9. Thompson, M. A. & Zerner, M. C. (1987) *J. Am. Chem. Soc.* **110**, 606–607.
10. Parson, W. W., Warshel, A. & Scherz, A. (1985) in *Antennas and Reaction Centers of Photosynthetic Bacteria, Structure, Interaction and Dynamics*, Springer Series in Chemical Physics, ed. Michele-Beyerle, M. E. (Springer, Berlin), Vol. 42, pp. 122–130.
11. Knapp, E. W., Scherer, P. O. J. & Fischer, S. F. (1986) *Biochim. Biophys. Acta* **852**, 295–305.
12. Parson, W. W. & Warshel, A. (1987) *J. Am. Chem. Soc.* **109**, 6152–6163.
13. Lavorel, J. (1957) *J. Phys. Chem.* **61**, 1600–1605.
14. Weber, G. & Teale, F. W. J. (1958) *Trans. Faraday Soc.* **54**, 640–648.
15. Katz, J. J. & Ballschmiter, K. (1968) *Angew. Chem.* **80**, 283–284.
16. Ballschmiter, K., Truesdell, K. & Katz, J. J. (1969) *Biochim. Biophys. Acta* **184**, 604–613.
17. Ballschmiter, K. & Katz, J. J. (1972) *Biochim. Biophys. Acta* **256**, 307–327.
18. Katz, J. J., Shipman, L. L., Cotton, T. M. & Janson, T. R. (1978) in *The Porphyrins*, ed. Dolphin, D. (McGraw-Hill, New York), Vol. 5, pp. 401–456.
19. Cotton, T. M., Loach, P. A., Katz, J. J. & Ballschmiter, K. (1978) *Photochem. Photobiol.* **27**, 735–749.
20. Katz, J. J. & Hindman, J. C. (1982) in *Events Probed by Ultrafast Laser Spectroscopy*, ed. Alfano, R. R. (Academic, New York), pp. 119–157.
21. Katz, J. J., Oettmeier, W. & Norris, J. R. (1976) *Philos. Trans. R. Soc. London B* **273**, 227–253.
22. Lutz, M., Robert, B., Zhow, Q., Newmann, J. M., Szponarski, W. & Berger, G. (1988) in *The Photosynthetic Bacterial Reaction Centers, Structure and Dynamics*, NATO ASI Series A: Life Sciences, eds. Breton, J. & Vermeglio, A. (Plenum, New York), Vol. 149, pp. 41–50.
23. Brown, S. B. & Shillcock, M. (1976) *Biochem. J.* **153**, 279–285.
24. Abraham, R. J., Goff, D. A. & Smith, K. M. (1988) *J. Chem. Soc. Perkins Trans.* **1**, 2443–2451.
25. Scherz, A., Rosenbach, V. & Malkin, S. (1985) in *Antennas and Reaction Centers of Photosynthetic Bacteria*, Springer Series in Chemical Physics, ed. Michel-Beyerle, M. E. (Springer, Berlin), Vol. 42, pp. 314–323.
26. Scherz, A. & Rosenbach-Belkin, V. (1988) in *The Photosynthetic Bacterial Reaction Centers, Structure and Dynamics*, NATO ASI Series A: Life Sciences, eds. Breton, J. & Vermeglio, A. (Plenum, New York), Vol. 149, pp. 295–308.
27. Rosenbach-Belkin, V. (1988) Ph.D. Thesis.
28. Scherz, A. & Rosenbach-Belkin, V. (1989) *Proc. Natl. Acad. Sci. USA* **86**, 1505–1509.
29. Scherz, A., Rosenbach-Belkin, V. & Fisher, J. R. E. (1989) in *Perspectives in Photosynthesis, Proceedings of the 22 Jerusalem Conference in Quantum Chemistry and Biology*, eds. Jortner, J. & Pullman, B. (Kluwer Press, Dodrecht), in press.
30. Gottstein, J. & Scheer, H. (1983) *Proc. Natl. Acad. Sci. USA* **80**, 2231–2234.
31. Fisher, J. R. E., Rosenback-Belkin, V. & Scherz, A. (1990) *Biophys. J.*, in press.
32. Hinton, J. F. & Harpool, R. D. (1977) *J. Am. Chem. Soc.* **99**, 349–353.
33. Renge, I. & Avarmaa, R. (1985) *Photochem. Photobiol.* **42**, 253–260.
34. Roth, M., Lewit-Bentley, A., Michel, H., Deisenhofer, J., Huber, R. & Oesterhelt, D. (1989) *Nature (London)* **340**, 659–662.
35. Rosenbach-Belkin, V., Braun, P., Kovatch, P. & Scherz, A. (1988) in *Photosynthesis Light-Harvesting Systems Organization and Function*, eds. Scheer, H. & Schneider, S. (de Gruyter, Berlin), pp. 323–337.
36. Kiley, P. J. & Kaplan, S. (1988) *Microbiol. Rev.* **52**, 50–69.
37. Eccles, J. & Honig, B. (1983) *Proc. Natl. Acad. Sci. USA* **80**, 4959–4962.
38. Kushner, L. M. & Hubbard, W. D. (1954) *J. Phys. Chem.* **58**, 1163–1167.
39. Rees, D. C., DeAntonio, L. & Eisenberg, D. (1989) *Science* **245**, 510–513.